CHEMISTRY JOURNAL OF MOLDOVA. General, Industrial and Ecological Chemistry. *2018, 13(1), 7-14*
ISSN (p) 1857-1727 ISSN (e) 2345-1688
http://cjm.asm.md
http://dx.doi.org/10.19261/cjm.2018.475

PLASMA-CHEMICAL SYNTHESIS OF SILVER NANOPARTICLES IN THE PRESENCE OF CITRATE

Margarita Skiba [a*], Alexander Pivovarov [a], Anna Makarova [a], Victoria Vorobyova [b]

[a]*Ukrainian State University of Chemical Technology, 8, Gagarina ave., Dnipro 49005, Ukraine*
[b]*National Technical University of Ukraine "Igor Sikorsky Kyiv Polytechnic Institute", 37, Peremohy ave., Kyiv 03056, Ukraine*
[*]*e-mail: Margaritaskiba88@gmail.com*

Abstract. The contact non-equilibrium low-temperature plasma technique is used to synthesize silver nanoparticles (AgNPs) employing trisodium citrate as capping agent. The AgNPs were characterized using UV-Vis spectroscopy, an absorption band at 400-440 nm confirmed nanoparticles formation. The effect of reaction conditions such as the concentration of silver ions, molar ratio Ag/citrate, irradiation time on the synthesis of AgNPs was studied. Characterization of AgNPs was carried out using scanning electron microscopy, X-ray diffraction and zeta potential analysis. The average size of formed silver particles was below 100 nm. XRD analysis revealed that the particles were face-centred cubic. The synthesized silver nanoparticles had significant antibacterial activity on two strains of Gram bacteria.

Keywords: nanoparticle, silver, stabilization, plasma, antibacterial.

Received: 06 March 2018/ Revised final: 17 April 2018/ Accepted: 25 April 2018

Introduction

Silver nanoparticles (AgNPs) are amongst the most extensively studied nanomaterials, which fascinate scientists due to their promising applications in optoelectronics [1-2], sensing [3-4], surface enhanced Raman scattering [5,6], catalysis [7-9] and others [10-12]. At the same time, silver nanoparticles can be applied in different ways: as individual silver nano-dispersions, as materials for purification and disinfection of water [12-13], as doping agent in films [14], corrosion inhibitor, *etc.* [15]. Hence, synthesis strategies that result in controlled NP size, distribution, shape and stability still represent an area of interest.

Different methods have been employed in the production of nano-sized metallic silver particles with different morphologies and sizes, for example, chemical reduction [16], electrochemical [16,17], photochemical [18,19], microwave-assisted [20], hydrothermal, laser ablation [21], sol-gel [22], sonochemical [16,23], green method [24,25]. One of the innovative and environmentally safe methods for preparation of nano-sized compounds is the use of plasma discharges of various configurations: plasma discharge generated between the electrodes immersed in liquid, at gas-liquid phase interface at reduced pressure, atmospheric pressure plasma in interaction with the liquid [26].

Among plasma-chemical discharges, contact non-equilibrium low-temperature plasma (CNP) is a promising option from the point of view of practical application [27]. Plasma discharge is generated between the electrode in the gaseous phase and the surface of the liquid where the other electrode is located. Therefore, chemical transformations at the phase interface are conditioned by the combined effect of electrochemical oxidation-reduction; initiated photolysis reactions, UV radiation; flow of charged particles from the gaseous phase to the surface of the liquid medium. By varying the composition of liquid phases it is possible, in some degree, to manage the paths of chemical transformations and composition of obtained products [28]. Previous research showed the efficiency of using the contact non-equilibrium low-temperature plasma in comparison with the conventional method of chemical reduction in solutions and photochemical deposition [29]. The efficiency of CNP use for synthesis of silver nanoparticles from the aqueous solutions of metal salts one-shot in the presence of sodium alginate is demonstrated in other published works [26]. Therefore, this synthesis technique seems to have potential for metal nanoparticles synthesis. The use of sodium alginate as capping agent may be inappropriate in some systems because of undesirable reaction [26]. Capping agents are

frequently used in colloidal synthesis to inhibit nanoparticle overgrowth and aggregation as well as to control the structural characteristics of the resulted nanoparticles in a precise manner. Citrate is the most popular capping agent of silver colloids that are lab-synthesized for general and specific applications; citrate coating serves both as a reducing agent and a stabilizer by decorating the particles with negative charges [30]. Therefore, studying of the process of obtaining silver nanoparticles in the presence of citrate, used as a stabilizing reagent, under the action of plasma discharge, is of scientific and practical interest.

The objective of this work is to obtain colloidal solutions of silver nanoparticles by using contact non-equilibrium low-temperature plasma and citrate as stabilizer.

Experimental

Materials

Silver nitrate (99.8%, Kishida), trisodium citrate, were purchased from Merck Co. Ltd. (Darmstadt, Germany). Aqueous solutions of silver nitrate at different concentration were prepared using ultrapure water (Direct-Q UV, Millipore) and were utilized as starting materials without further purification.

Synthesis of silver nanoparticles AgNPs

Silver nanoparticles were obtained in a synthesis reactor (Figure 1). $AgNO_3$ was dissolved in double distilled water to give a solution of 0.00025–0.003 mol/L. Then trisodium citrate was added to the $AgNO_3$ solution of different concentrations. Generally, 0.13 g trisodium citrate were added to 70 mL of 0.00025 mol/L (1); 0.0005 mol/L (2); 0.001 mol/L (3); 0.003 mol/L (4) aqueous silver nitrate solution under stirring for 6 seconds. These molar ratios Ag^+/citrate (0.05÷0.17) were chosen accordingly to already published reports [30,31]. The resulting reaction mixture was treated in the reactor with the discharge of contact non-equilibrium low-temperature plasma with fixed parameters (pressure, current strength, voltage). The electrodes were directly connected to the lines in order to apply voltage from the power sources and obtain the plasma discharge (the parameters of plasma I= 120 mA, P= 0.08 MPa). After plasma irradiation treatment, the resulted colloidal solutions were cooled at room temperature. The final product was obtained as a colloidal dispersion. The browning of the mixture of $AgNO_3$ indicated the synthesis of silver nanoparticles. The strong surface plasmon resonance (SPR) band at 400-440 nm in the UV–Vis spectra thus confirmed the formation of silver nanoparticles. The yield of silver nanoparticles was estimated by the difference between the concentration of silver ions in the initial solution and after plasma discharge treatment (using an "ELIS-131Ag" silver-selective electrode). The AgNPs obtained by plasma discharges were centrifuged at 5000 rpm for 5 min. The dried powders were then used for further characterization.

Equipment used for synthesis. The research was carried out at the Laboratory of Plasma-Chemical Technologies of the Ukrainian State University of Chemical Technology (Dnipro, Ukraine) on an installation of a discrete type with a reactor volume of 0.1 L (Figure 1).

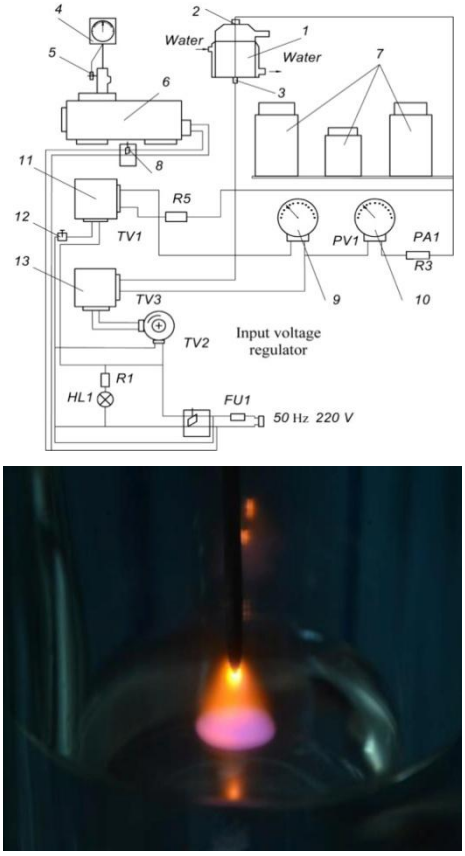

Figure 1. The circuit diagram and photo discharge of the installation for plasma-chemical treatment of water solutions: *1* – reactor; *2, 3* – electrodes; *4* – vacuum gauge; *5* – crane; *6* – pump; *7* – filtering elements; *8* – switch; *9* – voltmeter; *10* – ammeter; *11* – firearm transformer; *12* – switch; *13* – voltage transformer.

Cathode (diameter 4 mm, 18H10T stainless steel electrodes) was located in the liquid part, with the anode (diameter 2.4 mm) placed at the distance of 10 mm from the surface of solution. Volume of solution in the reactor was equal to 70 mL. Cooling of reaction mixture was ensured by

continuous circulation of cold water. Pressure in the reactor was maintained at 80±4 kPa. The voltage of 500–1000 V was applied to the electrodes to obtain the plasma discharge. The current strength was maintained at the level of 120±6 mA. Duration of plasma processing of solutions ranged from 1 to 5 min.

Characterization techniques

UV-Vis spectra of colloidal solutions were recorded in the wavelength range of 190-700 nm using the UV-5800PC spectrophotometer (FRU, China) and quartz cuvettes.

Zeta potential of colloidal solutions was measured on a Zetasizer Nano-25 analyzer (Malvern Instruments Ltd., Malvern, England).

Microphotographs of nanoparticles were obtained using the scanning microscope JEOL JSM-6510LV (JEOL, Tokyo, Japan).

X-ray diffraction patterns were registered using the X-ray diffractometer Ultima IV Rigaku. The size of the AgNPs (D, crystallite size) were estimated from the Debye–Scherrer Eq.(1) [32].

$$D = \frac{0.9\lambda}{\beta \cos\theta} \quad (1)$$

where, β is FWHM (full width at half maximum);
θ is the angle of diffraction;
wavelength (λ) for X-ray is 0.1541 nm.

Antibacterial assay

The disk diffusion method was used to study the antibacterial activity of the synthesized silver nanoparticles. *Staphylococcus aureus* (ATCC 25923) and *Escherichia coli* (ATCC 35218) were used as model test strains for Gram-positive and Gram-negative bacteria, respectively. The bacterial suspension (About 10^4 colony forming units (CFUs) of freshly cultured microbial cells) was spread on nutrient agar in a Petri plate to create confluent lawn of bacterial growth. The wells of 5 mm were prepared by borer. The solutions of different AgNPs concentrations (15 μL) were poured into each well. The well without silver nanoparticles was treated as blank (water). After 24 h incubation at 37°C, the dimensions of the inhibition zones around the samples were measured in five directions, and the average values were used to calculate the circle zone area.

Results and discussion

The UV-Vis spectrophotometric technique was applied to confirm the formation of silver nanoparticles in the CNP plasma-irradiated $AgNO_3$/citrate solution. It is a well known fact that colloidal silver nanoparticles exhibit absorption in the wavelength range from 380 to 450 nm depending on the complex dielectric constant of the metal, the cluster size and the environment [31,33].

Figure 2 shows the absorption spectra of the Ag solutions obtained at various $AgNO_3$ concentrations studied in the range 0.00025–0.003 mol/L without and in the presence of fixed concentration of citrate (the parameters of plasma I= 120 mA, P= 0.08 MPa, τ= 5 min *(a)* and τ= 4 min *(b)*).

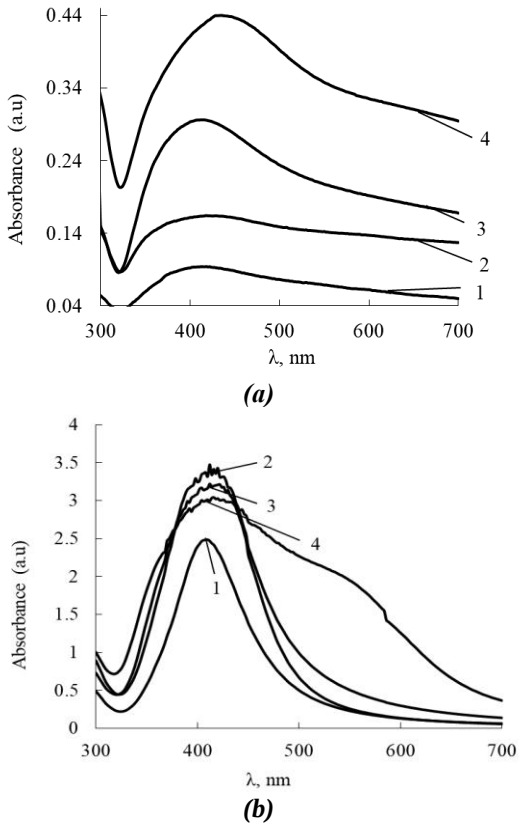

Figure 2. The UV-Vis spectra of AgNPs *(a)* and AgNPs/citrate *(b)* prepared by discharge plasma at various concentrations of $AgNO_3$: *1* – 0.00025 mol/L; *2* – 0.0005 mol/L; *3* – 0.001 mol/L; *4* – 0.003 mol/L.

Figure 2*(a)* shows that silver nanoparticles are formed due to the plasma discharge action, even in the absence of the citrate ions (maximum of absorption SPR (λ_{max}) at 440 nm). UV-Vis spectra presented in Figure 2*(b)* show that treatment of the silver nitrate/citrate solution by low-temperature plasma discharge on the spectrum results in the SPR absorption peak (λ_{max}) at 408–420 nm, characterizing the formation of silver nanoparticles. Therefore, the introduction of capping agent promotes the increase in intensity of formation of silver nanoparticles. From the Figure 2*(b)*, a redshift from 408 nm to 420 nm and spectral broadening with increase

concentration of $AgNO_3$ is observed. Also, the absorption peak intensity gradually increases with the increase of $AgNO_3$ concentration to 0.0005 mol/L reflecting the formation of more AgNPs [34,35]. This indicates a slight increase of the size of formed particles (up to 5 nm). Thus it can be assumed, that although the silver nitrate concentration is increased, the particle size does not increase much, possibly due to the capping action of citrate. The increase in the concentration of silver ions (more than 0.0005 mol/L) leads to a slight decrease of the peak intensity (0.003–0.001 mol/L curves *1-3*) and there is obvious absorption in the range of 450–600 nm indicating that negligible aggregation occurs in this reactive system and the nanoparticles are well dispersed (at 0.003 mol/L).

Figure 3 shows the absorption spectra of the silver solutions obtained at various $AgNO_3$ concentrations 0.00025–0.003 mol/L in the presence of fixed concentration of citrate and different duration of irradiation.

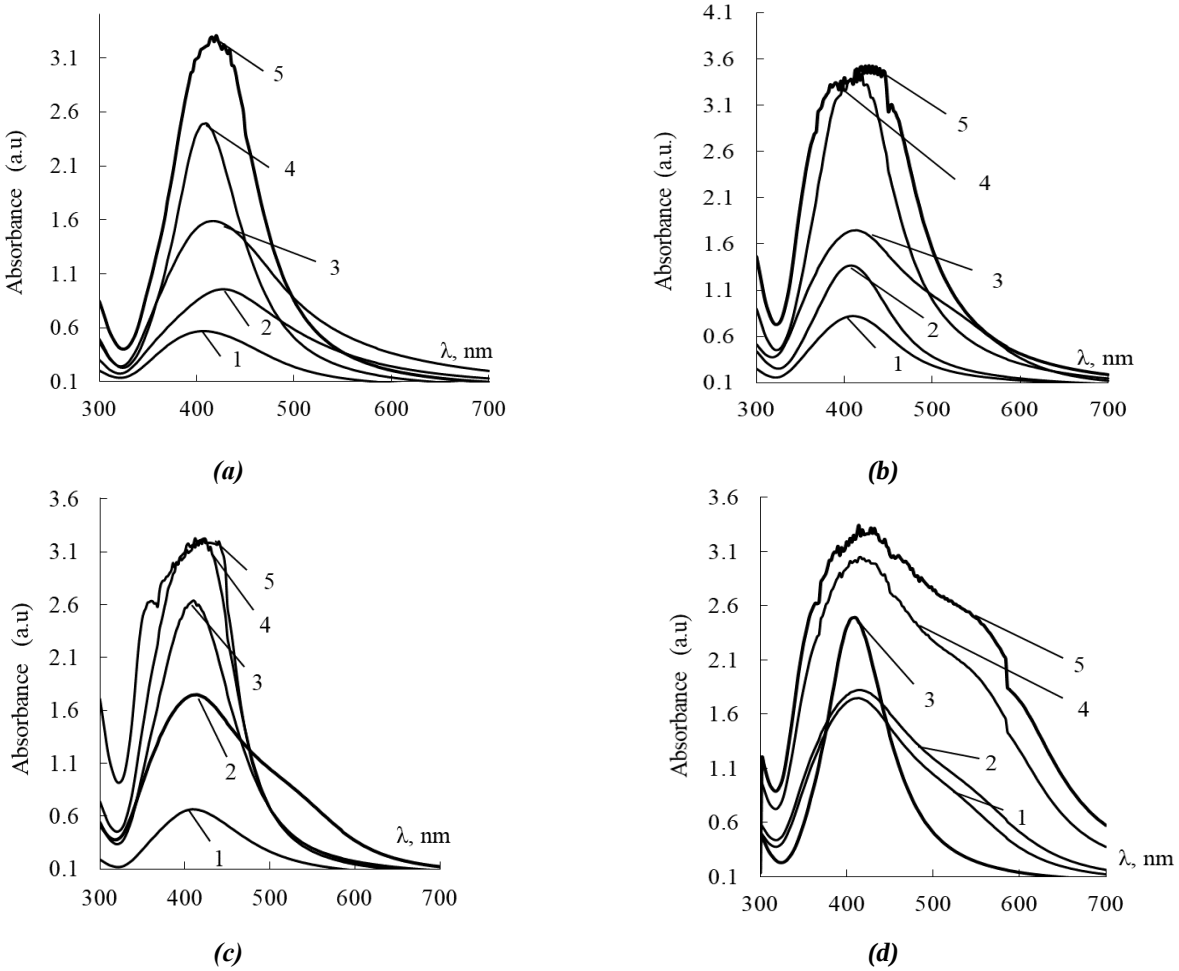

Figure 3. UV–Vis spectra of aqueous solution $AgNO_3$/citrate treated with plasma at different discharge durations *1* – 1 min; *2* – 2 min; *3* – 3 min; *4* – 4 min; *5* – 5 min, for various concentrations of Ag^+ ions *(a)* 0.00025 mol/L; *(b)* 0.0005 mol/L; *(c)* 0.001 mol/L; *(d)* 0.003 mol/L.

Zeta potential measurements were conducted to evaluate the stability of the silver suspensions (Figure 4). The zeta potential is based on the mobility of a particle in an electric field and is related to the electrical potential at the junction between the diffuse ion layer surrounding the particle surface and the bulk solution. Generally, a suspension that exhibits a zeta potential less than –20 mV is considered unstable and will result in particles settling out of solution in the absence of other factors. At different initial concentration of Ag^+ in solution without stabilizer, there was little variation in the zeta potential value of AgNPs, indicating low stability of the synthesized nanoparticles. Overall, all obtained samples solutions of silver nanoparticles/citrate depending on the initial Ag^+ and concentration of stabilizer are characterized by an average value of zeta potential in the range from –28.2 mV to –32.0 mV, which is typical of the stable colloidal systems [36].

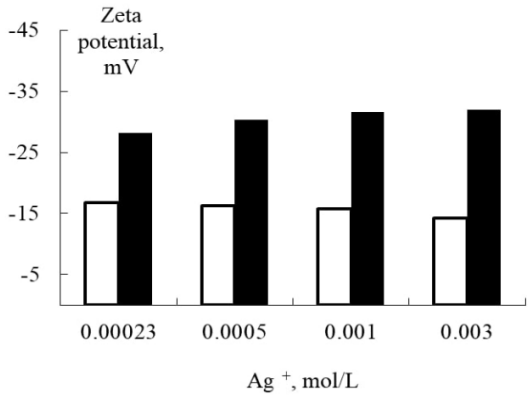

Figure 4. Dependence of zeta potential (mV) colloidal solution of silver prepared by discharge plasma on various concentration of Ag^+ (mol/L) without using capping agent (white bar) and with citrate (black bar).

The AgNPs sample obtained in the experimental conditions: the parameters of plasma I= 120 mA, P= 0.08 MPa, τ= 4 min; C(Ag^+)=0.003 mol/L was investigated using the powder X-ray diffraction (XRD) method and SEM microscopy. Figure 5 shows typical XRD pattern of silver nanoparticles obtained in an aqueous solution: peaks at 2Θ values of 38.1, 44.9, 77.5° are attributed to the (111), (200), (311) crystalline planes of the face centered cubic crystalline structure of metallic silver. The intensity of peaks reflected a high degree of crystallinity of silver nanoparticles. The diffraction peaks are broad, which indicates that the crystallite size is very small [32]. The calculated particle size (crystallite size) details are in Table1. The average crystallite size calculated using Debye-Scherrer formula (Eq.(1)) for (111, 200, 311) plane of AgNPs were 6.0 – 28.2 nm.

Table 1

The size of silver nanoparticles.

2Θ, °	*crystalline planes, hkl*	*β*	*D, nm*
38.1	(111)	0.005	28.2
44.9	(200)	0.010	12.0
77.5	(311)	0.029	6.0

A comparison of the (111), (200), (220) diffraction intensities reveals features that are intrinsically related to the shapes of the particles being examined. For the Ag /citrate nanoparticles prepared by discharge plasma, the intensity ratio between the (200) and the (111) indicated the formation of icosahedron type of nanocrystals [32,37].

The SEM image of the prepared Ag/citrate is shown in Figures 6. The obtained SEM image indicates that nanoparticles are relatively spherical (visual observation) of an average diameter up to 100 nm (linear dimensional scale). The size distribution of AgNPs is presented in Figure 7. According to the obtained distribution, the size of the AgNPs is in the range 35–100 nm, being comparable with SEM data.

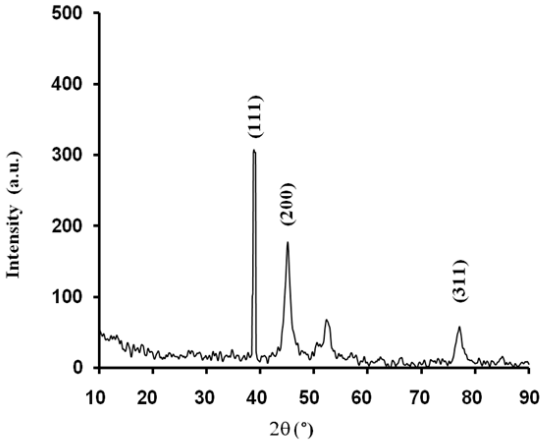

Figure 5. X-ray diffraction pattern of AgNPs/citrate prepared by discharge plasma.

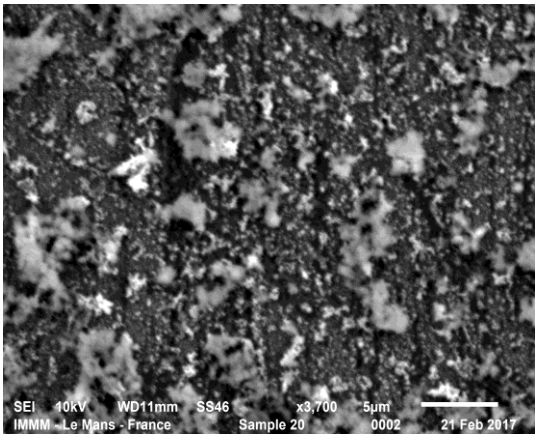

Figure 6. SEM-image of AgNPs/citrate prepared by discharge plasma.

It is commonly known and well established that silver nanoparticles show antibacterial activity [38]. The plasma chemical synthesized AgNPs (with 0.00025–0.003 mol/L/citrate) were studied for their antibacterial activity. The obtained results (Table 2) show that antibacterial activity is exclusively due to AgNPs. There is good antibacterial activity against both Gram-negative and Gram-positive bacteria observed, but it shows higher antibacterial activity against (*Escherichia coli*) (Gram-negative) then (*Staphylococcus aureus*) (Gram-positive) (Table 2). The zone of inhibition increases with the increase in AgNPs concentration. The blank sample shows no zone of inhibition, which indicates that antibacterial activity is exclusively due to AgNPs.

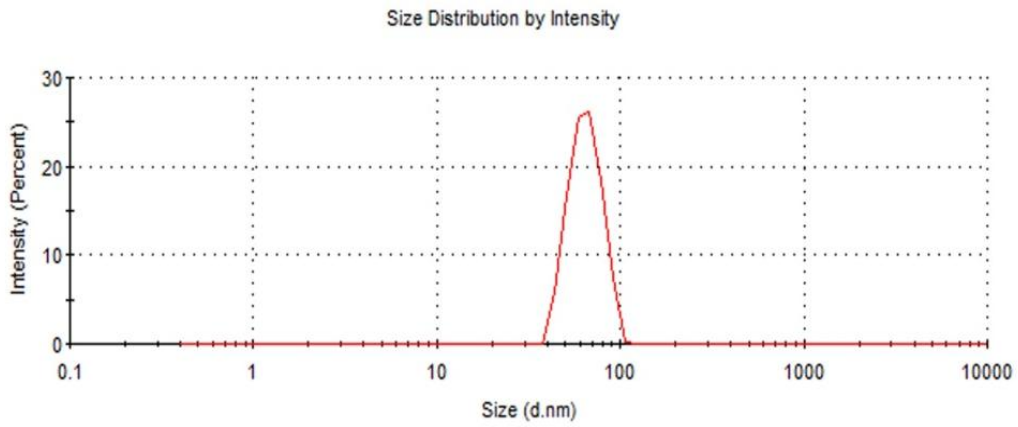

Figure 7. Size distribution of silver/citrate nanoparticles obtained by discharge plasma.

Table 2

Zone of inhibition of synthesized silver nanoparticles against bacterial strains.

Tested bacterial strains	*Zone of inhibition by AgNPs, mm*			
	Blank	*Ag^+/citrate, mol/L*		
		0.00025	0.001	0.003
Escherichia coli	0	10	20	25
Staphylococcus aureus	0	3	5	11

The differential sensitivity of Gram-negative and Gram-positive bacteria toward AgNPs is possible due to the difference in their structure of the cell wall. The cell wall of the Gram-positive bacteria is composed of a thick layer of peptidoglycan, consisting of linear polysaccharide chains cross-linked by short peptides thus forming a more rigid structure leading to difficult penetration of the silver nanoparticles, but the cell walls of Gram-positive bacteria possess a thinner layer of peptidoglycan [39].

Conclusions

Silver nanoparticles were prepared in aqueous $AgNO_3$ solution by using contact non-equilibrium low-temperature plasma and trisodium citrate as capping agent. The formation of silver nanoparticles in the presence of capping agent is demonstrated by the presence of the peak λ_{max} = 408–420 nm in the UV-Vis spectra.

The obtained results show that the introduction of capping agent promotes formation of silver nanoparticles. The increase in silver nitrate concentration does not increase the size of the nanoparticles. The concentration of silver nanoparticles increases with the increase of duration of plasma action on the solution. The formation of silver nanoparticles was confirmed by X-ray diffraction. The average size of formed silver particles is below 100 nm. The synthesized silver nanoparticles had significant antibacterial activity against *Escherichia coli* and *Staphylococcus aureus* strains.

Acknowledgments

This work was supported by a grant of the Ministry of education and science of Ukraine (grant number 2044, 2016–2018) and program European Union (Harmonising water related graduate education /WaterH www.waterh.net).

References

1. Hu, X.; Chan C.T. Photonic crystals with silver nanowires as a near-infrared superlens. Applied Physics Letters, 2004, 85(9), pp. 1520-1522. DOI: https://doi.org/10.1063/1.1784883
2. Alshehri, A.H.; Jakubowska, M.; Młożniak, A.; Horaczek M.; Rudka, D.; Free, Ch.; Carey, J.D. Enhanced electrical conductivity of silver nanoparticles for high frequency electronic applications. Applied Materials & Interfaces, 2012, 4(12), pp. 7007-7010. DOI: https://doi.org/10.1021/am3022569
3. Cobley, C.M.; Skrabalak, S.E.; Campbell, D.J.; Xia, Y. Shape-controlled synthesis of silver nanoparticles for plasmonic and sensing applications. Plasmonics, 2009, 4(2), pp. 171-179. DOI: https://doi.org/10.1007/s11468-009-9088-0
4. Nguyen, N.D.; Nguyen, T.V.; Chu, A.D.; Tran, H.V.; Tran, L.T.; Huynh, Ch.D. A label-free colorimetric sensor based on silver nanoparticles

directed to hydrogen peroxide and glucose. Arabian Journal of Chemistry, 2018, pp. 1-10. DOI: https://doi.org/10.1016/j.arabjc.2017.12.035
5. Li, Zh.; Wang, M.; Jiao, Y.; Liu, A.; Wang, Sh.; Zhang, Ch.; Yang, Ch.; Xu, Y.; Li, Ch.; Man, B. Different number of silver nanoparticles layers for surface enhanced Raman spectroscopy analysis. Sensors and Actuators B: Chemical, 2018, 255, pp. 374-383. DOI: https://doi.org/10.1016/j.snb.2017.08.082
6. Tao, L.; Lou, Y.; Zhao, Y.; Hao, M.; Yang, Y.; Xiao, Y.; Tsang, Y.H.; Li, J. Silver nanoparticle-decorated graphene oxide for surface-enhanced Raman scattering detection and optical limiting applications. Journal of Materials Science, 2018, 53(1), pp. 573–580. DOI: https://doi.org/10.1007/s10853-017-1501-z
7. Ajitha, B.; Kumar Reddy, Y.Ash.; Jeon H.-J.; Ahn, W.Ch. Synthesis of silver nanoparticles in an eco-friendly way using *Phyllanthus amarus* leaf extract: Antimicrobial and catalytic activity. Advanced Powder Technology, 2018, 29(1), pp. 86-93. DOI: https://doi.org/10.1016/j.apt.2017.10.015
8. Young, J.; Cheng, K.; Young, Y.; Chen, X.; Chen, Y.; Chang, T.; Yen, H.; Chen, Ch. Chondroitin sulfate-stabilized silver nanoparticles: Improved synthesis and their catalytic, antimicrobial, and biocompatible activities. Carbohydrate Research, 2018, 457, pp. 14-24. DOI: https://doi.org/10.1016/j.carres.2017.12.004
9. Asharani, I.V.; Thirumalai, D.; Sivakumar, A. Dendrimer encapsulated silver nanoparticles as novel catalysts for reduction of aromatic nitro compounds. IOP Conference Series: Materials Science and Engineering, 2017, 263, pp. 1-7. DOI: https://doi.org/10.1088/1757-899X/263/2/022010
10. Franci, G.; Falanga, A.; Galdiero, S.; Palomba, L.; Rai, M.; Morelli, G.; Galdiero, M. Silver nanoparticles as potential antibacterial agents. Molecules, 2015, 20(5), pp. 8856-8874. DOI: https://doi.org/10.3390/molecules20058856
11. Liu, C.X.; Zhang, D.R.; He, Yi; Zhao, X.S.; Bai, R. Modification of membrane surface for anti-biofouling performance: Effect of anti-adhesion and anti-bacteria approaches. Journal of Membrane Science, 2010, 346(1), pp. 121-130. DOI: https://doi.org/10.1016/j.memsci.2009.09.028
12. Cruz, M.C.; Ruano, G.; Wolf, M.; Hecker, D.; Vidaurre, E.C.; Schmittgens, R.; Rajal, V.B. Plasma deposition of silver nanoparticles on ultrafiltration membranes: Antibacterial and anti-biofouling properties. Chemical Engineering Research and Design, 2015, 94, pp. 524-537. DOI: https://doi.org/10.1016/j.cherd.2014.09.014
13. Furlan, P.Y.; Fisher, A.J.; Melcer, M.E. Furlan, A.Y.; Warren, J.B. Preparing and testing a magnetic antimicrobial silver nanocomposite for water disinfection to gain experience at the nanochemistry–microbiology interface. Journal of Chemical Education, 2017, 94(4), pp. 488-493. DOI: https://doi.org/10.1021/acs.jchemed.6b00692
14. Sahu, D.; Sarkar, N.; Sahoo, G.; Mohapatra, P.; Swain, S.K. Nano silver imprinted polyvinyl alcohol nanocomposite thin films for Hg^{2+} sensor. Sensors and Actuators B: Chemical, 2017, 246, pp. 96-107. DOI: https://doi.org/10.1016/j.snb.2017.01.038
15. Solomon, M.M.; Umoren, S.A. Performance assessment of poly (methacrylic acid)/silver nanoparticles composite as corrosion inhibitor for aluminium in acidic environment. Journal of Adhesion Science and Technology, 2015, 29(21), pp. 2311-2333. DOI: https://doi.org/10.1080/01694243.2015.1066235
16. Abou El-Nour, K.M.M.; Eftaiha, A.; Al-Warthan, A.; Ammar, R.A. Synthesis and applications of silver nanoparticles. Arabian Journal of Chemistry, 2010, 3(3), pp. 135-140. DOI: https://doi.org/10.1016/j.arabjc.2010.04.008
17. Iravani, S.; Korbekandi, H; Mirmohammadi, S.V; Zolfaghari, B. Synthesis of silver nanoparticles: chemical, physical and biological methods. Research in Pharmaceutical Sciences, 2014, 9(6), pp. 385-406. https://www.ncbi.nlm.nih.gov/pmc/articles/PMC4326978/
18. Xie, P.; Ji, W.; Wei, Zh. Preparation and properties of silver nanoparticles. Characterization and Application of Nanomaterials, 2018, 1, pp. 40-48. http://systems.enpress-publisher.com/index.php/CAN/article/view/239
19. Alarcon, E.I; Udekwu, K.; Skog, M; Pacioni, N.L.; Stamplecoskie, K.G.; González-Béjar, M.; Polisetti, N.; Wickham, A.; Richter-Dahlfors, A.; Griffith, M; Scaiano, J.C. The biocompatibility and antibacterial properties of collagen-stabilized, photochemically prepared silver nanoparticles. Biomaterials, 2012, 33(19), pp. 4947-4956. DOI: https://doi.org/10.1016/j.biomaterials.2012.03.033
20. Francis, S.; Joseph, S.; Ebey, P.K.; Beena M. Microwave assisted green synthesis of silver nanoparticles using leaf extract of *Elephantopus scaber* and its environmental and biological applications. Journal Artificial Cells, Nanomedicine, and Biotechnology, 2017, 46(4), pp. 795-804. DOI: https://doi.org/10.1080/21691401.2017.1345921
21. Verma, Sh.; Rao, B.T.; Srivastava, A.P.; Srivastava, D.; Kaul, R.; Singh, B. A facile synthesis of broad plasmon wavelength tunable silver nanoparticles in citrate aqueous solutions by laser ablation and light irradiation. Colloids and Surfaces A: Physicochemical and Engineering Aspects, 2017, 527, pp. 23-33. DOI: https://doi.org/10.1016/j.colsurfa.2017.05.003
22. Iconaru, S.L.; Chapon, P.; Coustumer, Ph.L.; Predoi, D. Antimicrobial activity of thin solid films of silver doped hydroxyapatite prepared by sol-gel method. The Scientific World Journal, 2014, 8 p. DOI: http://dx.doi.org/10.1155/2014/165351
23. Elsupikhe, R.F.; Shameli, K.; Ahmad, M.B.; Ibrahim, N.A.; Zainudin, N. Green sonochemical synthesis of silver nanoparticles at varying

concentrations of κ-carrageenan. Nanoscale Research Letters, 2015, 10(302), pp.1-8. DOI: https://doi.org/10.1186/s11671-015-0916-1

24. Asghar, M.A.; Zahir, E.; Shahid, S.M.; Khan, M.N.; Asghar, M.A.; Iqbal, J.; Walker, G. Iron, copper and silver nanoparticles: Green synthesis using green and black tea leaves extract and evaluation of antibacterial, antifungal and aflatoxin B_1 adsorption activity. LWT – Food Science and Technology, 2018, 90, pp. 98-107. DOI: https://doi.org/10.1016/j.lwt.2017.12.009
25. Remya, V.R.; Abitha, V.K.; Rajput, P.S.; Rane, A.V.; Dutta, A. Silver nanoparticles green synthesis: A mini review. Chemistry International, 2017, 3(2), pp. 165-171. http://bosaljournals.com/chemint/index.php/10-issue-2
26. Saito, G.; Akiyama, T. Nanomaterial synthesis using plasma generation in liquid. Journal of Nanomaterials, 2015, 21 p. DOI: http://dx.doi.org/10.1155/2015/123696
27. Pivovarov, A.A.; Kravchenko, A.V.; Tishchenko, A.P. Nikolenko, N.V.; Sergeeva, O.V.; Vorob'eva, M.I.; Treshchuk, S.V. Contact nonequilibrium plasma as a tool for treatment of water and aqueous solutions: Theory and practice. Russian Journal of General Chemistry, 2015, 85(5), pp. 1339-1350. (in Russian). DOI: 10.1134/S1070363215050497
28. Skiba, M.; Pivovarov, A.; Makarova, A.; Pasenko, O.; Khlopytskyi, A.; Vorobyova, V. Plasma-chemical formation of silver nanodisperssion in water solutions. Eastern-European Journal of Enterprise Technologies, 2017, 6(6), pp. 59-65. DOI: https://doi.org/10.15587/1729-4061.2017.118914
29. Pivovarov, O.A.; Skiba, M.I.; Makarova, A.K.; Vorobyova, V.I.; Pasenko, O.O. Preparation of silver nanoparticles by contact nonequilibrium low-temperature plasma in the presence of sodium alginate. Issues of Chemistry and Chemical Technology, 2017, 6, pp. 82-88. http://oaji.net/articles/2017/1954-1513761696.pdf
30. Sharma, V.K.; Siskova, K.M.; Zboril, R.; Gardea-Torresdey, J.L. Organic-coated silver nanoparticles in biological and environmental conditions: Fate, stability and toxicity. Advances in Colloid and Interface Science, 2014, 204, pp. 15-34. DOI: https://doi.org/10.1016/j.cis.2013.12.002
31. Bastús, N.G.; Merkoçi, F.; Piella, J.; Puntes, V. Synthesis of highly monodisperse citrate-stabilized silver nanoparticles of up to 200 nm: kinetic control and catalytic properties. Chemistry of Materials, 2014, 26 (9), pp. 2836-2846. DOI: https://doi.org/10.1021/cm500316k
32. Seo D.; Yoo C.; Chung I.S.; Park S.M.; Ryu S.; Song H. Shape adjustment between multiply twinned and single-crystalline polyhedral gold nanocrystals: decahedra, icosahedra, and truncated tetrahedra. The Journal of Physical Chemistry C, 2008, 112 (7), pp. 2469-2475. DOI: 10.1021/jp7109498
33. Baetzold, R.C. Silver–water clusters: a theoretical description of $Ag_n (H_2O)_m$ for n= 1–4; m= 1–4. The Journal of Physical Chemistry C, 2015, 119(15), pp. 8299-8309. DOI: 10.1021/jp512556g
34. Bhui, D.K.; Bar, H.; Sarkar, P.; Sahoo, G.P.; De, S.P.; Misra, A. Synthesis and UV-Vis spectroscopic study of silver nanoparticles in aqueous SDS solution. Journal of Molecular Liquids, 2009, 145(1), pp. 33-37. DOI: https://doi.org/10.1016/j.molliq.2008.11.014
35. Smitha, S.L.; Nissamudeen, K.M.; Philip D.; Gopchandran K.G. Studies on surface plasmon resonance and photoluminescence of silver nanoparticles. Spectrochimica Acta Part A: Molecular and Biomolecular Spectroscopy, 2008, 71 (1), pp. 186-190. DOI: https://doi.org/10.1016/j.saa.2007.12.002
36. Bac, L.H.; Gu, W.H.; Kim, J.C.; Kim, J.S. Characterization and stability of silver nanoparticles in aqueous solutions. Journal of Korean Powder Metallurgy Institute, 2012, 19(1), pp. 55-59. DOI: https://doi.org/10.4150/KPMI.2012.19.1.055
37. Kim, F.; Connor, S.; Song, H.; Kuykendall, T.; Yang, P. Platonic gold nanocrystals. Angewandte Chemie International Edition, 2004, 43(28), pp. 3673-3677. DOI: https://doi.org/10.1002/anie.200454216
38. Silva, L.P.; Silveira, A.P.; Bonatto, C.C.; Reis, I.G.; Milreu, P.V. Silver nanoparticles as antimicrobial agents: past, present, and future. Nanostructures for Antimicrobial Therapy, 2017, pp. 577-596. DOI: https://doi.org/10.1016/B978-0-323-46152-8.00026-3
39. Zhao, X.; Xia, Y.; Li, Q.; Ma, X.; Quan, F.; Geng, C.; Han, Zh. Microwave-assisted synthesis of silver nanoparticles using sodium alginate and their antibacterial activity. Colloids and Surfaces A: Physicochemical Engineering Aspects, 2014; 444, pp. 180-188. DOI: https://doi.org/10.1016/j.colsurfa.2013.12.008.